

# Effect of distribution of yield-shear-force-coefficient on the probabilistic seismic safety of existing tall buildings

S. H. Zhang, J. Kanda & R. Iwasaki  
*University of Tokyo, Japan*

**ABSTRACT:** A second-moment reliability analysis is applied to evaluate the probability seismic safety of existing tall buildings in Japan. Effects of the seismic hazard, of the base shear force coefficient and of the yield-shear-force coefficient distribution on the seismic safety margin index are discussed.

## 1. INTRODUCTION

Dynamic analyses are commonly carried out in the seismic design for tall buildings in Japan. Although there is a general specified rule for the input motions and the response criteria, the seismic safety for all buildings may not be necessarily uniform. Particularly probabilistic evaluation of the seismic safety may well lead to wide variations. It is important to find out causes for such variation. Among many parameters used to analyze the seismic safety, the seismic hazard, the base shear force coefficient and the distribution of yield shear force coefficient are considered to be significant ones. Based on the statistical examination of the dynamic characteristics of existing Japanese tall buildings in recent years, the distribution of yield shear force coefficient can be classified into three patterns. Effects of these distributions on the seismic safety in terms of the second moment reliability proposed by one of the authors are examined and the significance is subsequently demonstrated.

## 2. METHOD

### 2.1 Models for analysis

In Japan the vertical distribution of yield-shear-force coefficient  $C_{Ri}$  for ordinary buildings is specified in a form normalized by the base-shear-coefficient  $C_{Ri}A_i$  by the so-called  $A_i$  distribution in the Building Standard Law (BSL), 1986. Statistical examinations on design parameters of recent existing Japanese tall buildings revealed that the distributions can be classified into three patterns irrespective of the construction types of structures. They are: pattern S (smaller than the  $A_i$  distribution in most stories), pattern M (approximately equal to the  $A_i$  distribution) and pattern L (greater than

the  $A_i$  distribution in most stories)(Zhang, 1990).

Nine examples from the steel structure (S) and nine from the steel reinforced concrete structure (SRC) and six from the reinforced concrete structure (RC) are chosen as typical cases in this study. In order to reduce the inelastic response computation time, models are simplified into 6-lumped-mass system (Zhang, 1991). The accuracy of this model was fully examined by comparing the responses with those of the original models used in the design procedure.

The distributions for all examples are shown in Fig. 1 in terms of the ratio of the normalized yield-shear-force coefficient distribution to  $A_i$  versus the relative vertical position.

### 2.2 Simulated input motions and seismic hazard

In order to evaluate the response in the inelastic range simulated earthquake ground motions were used as input motions.

Ten simulated earthquake ground motions, with the Kanai-Tajimi spectrum (Kanai, 1961) and Jennings' envelope function (Jennings, 1968), for earthquake magnitude  $M=8.5$ , are generated by the use of random phase angles. The power spectrum  $S_g(f)$  is given by

$$S_g(f) = S_0 \frac{1 + 4\xi_g^2 \left(\frac{f}{f_g}\right)^2}{\left[1 - \left(\frac{f}{f_g}\right)^2\right]^2 + 4\xi_g^2 \left(\frac{f}{f_g}\right)^2} \quad (1)$$

where  $S_0$ : spectrum intensity;  $f_g$ : predominant frequency;  $\xi_g$ : damping ratio. As a typical ground condition  $\xi_g = 0.47$ ,  $f_g = 3\text{Hz}$  (Kanda et al, 1987) are assumed.

Seismic hazard is described by the mean value  $\bar{a}$  (m/s<sup>2</sup>) of 50-year maximum peak ground acceleration on the

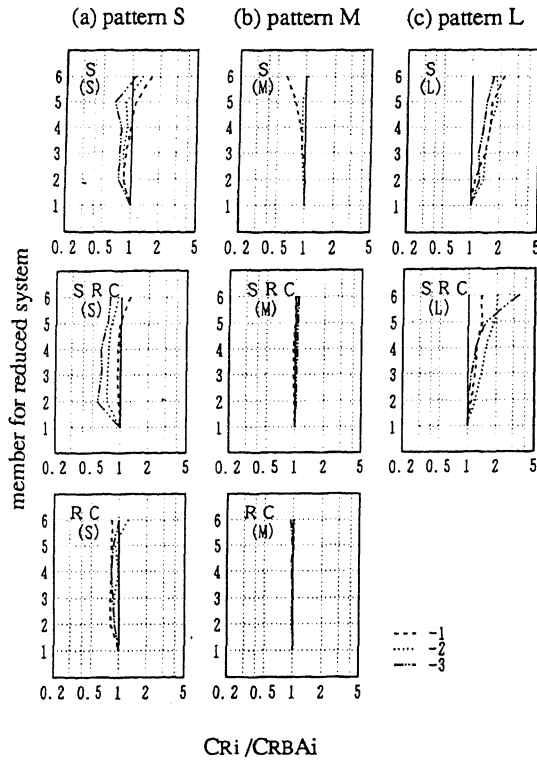


Fig.1 Ratio of the distribution of normalized yield-shear-force coefficient to the  $A_i$  distribution

ground surface. It is obtained from the mean of 50-year maximum of bedrock velocity (m/s) multiplied by 47, according to a proposal by Dan et al,1986.

### 2.3 Equivalent elastic response

At first response calculation is carried out for the simulated motion with small accelerations so that the maximum response of the model remains in the elastic range. The acceleration, corresponding to the first break point on the restoring force characteristics, is determined and taken as the reference input level  $a_0$ . At the level  $a_0$  multiplied by  $n$  ( $n=1,2,3,4$  for the examples with S structure and S type from the SRC structure, where S type is defined as that the first break of the skeleton curve corresponds to the yielding point.  $n=1, 4, 8, 12$  for the examples with RC structure and RC type in the SRC structure, where RC type is defined as the first break of the skeleton curve corresponds to the crack point of concrete). We carry out elastic-plastic response computations at four steps with ten motions for each model. The model's restoring force characteristics are taken from the design documents.

The inelastic response ( $Q, D$ ) is converted into the energy equivalent elastic response  $Q^*$ , as defined in Fig.2, where the area oabcd is equal to that of odef. The first break is point ( $Q_y, D_y$ ) for S type and ( $Q_c, D_c$ ) for RC type.

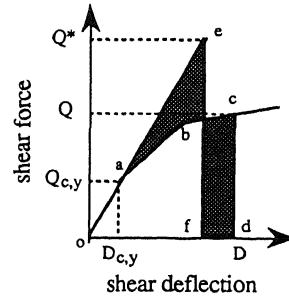


Fig.2 Definition of equivalent elastic response

### 2.4. Definition of ultimate limit state

The ductility factor  $\mu$  is used here to define the ultimate limit state index.  $\mu$  is obtained by dividing the maximum displacement by  $D_y$  (the first break point in S type and second break point for RC type). Then the mean ultimate limit state is assumed to correspond following  $\mu$  values in this study; for S structure  $\mu = 4.0$ , for SRC structure  $\mu = 3.0$ , for RC structure  $\mu = 2.0$ .

### 2.5 Seismic margin index $\beta$

The seismic margin index  $\beta$  is a second moment reliability index proposed by Kanda et al,1988. Based on the approximate linear relation between the equivalent elastic response,  $Q^*$  and the input acceleration  $a$ , as shown in Fig.3.

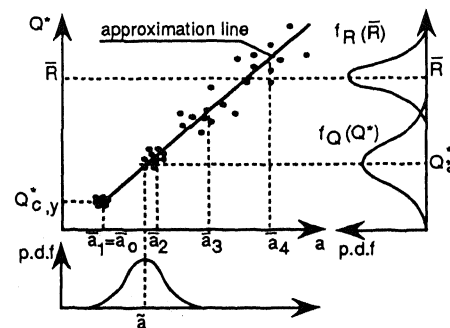


Fig.3 Conceptual diagram for the transformation from the earthquake intensity to the load effect

$$\beta = \frac{\ln m_R - \frac{\zeta_R^2}{2} + \frac{\ln m_R}{\ln m_a} \left( \frac{\zeta_a^2}{2} + \ln \frac{a_0}{\tilde{a}} \right)}{\sqrt{\zeta_R^2 + \left( \frac{\ln m_R}{\ln m_a} \zeta_a \right)^2}} \quad (2)$$

where  $m_R$  is the resistance margin defined as the ratio of the mean of ultimate resistance of the member,  $\bar{R}$ , to the mean of elastic response for the reference input level  $a_0$ ,  $m_a$  is the input intensity margin defined as  $a_R/a_0$ ;  $a_R$  is the level causing equivalent elastic response equal to  $\bar{R}$ ,  $a_0$  is the reference input level and  $\zeta_x^2 = \ln(1 + V_x^2)$ , where  $V_x$  is the coefficient of variation of random variable  $x$ .

### 3. Probabilistic Evaluation of Seismic Safety

Some parameter used in models are listed in Table 1. where  $C_{RB}$  is the yield shear force coefficient in design,  $C_{DB}$  is the design base shear force coefficient determined based on BSL formulae, although BSL formulae do not generally apply to tall buildings with the height over 60m. The coefficients of variation for earthquake load and resistance are assumed as 60% and 10% respectively.

#### 3.1 Vertical distribution of $\beta$

In order to examine the relation between  $C_{Ri}$  distribution and  $\beta$  distributions of  $\beta$  are shown in Fig.4 for each pattern of yield-shear-force coefficient distribution.  $\beta$ -values for S and SRC structures are in the range of 4 to 6, while for RC structures it varies from 4 to 5.

From comparison of Fig.4 with Fig.1, the vertical distribution of  $\beta$  does not exactly correspond to  $C_{Ri}$  distribution. Nevertheless there is a general tendency such that the minimum of  $\beta$  appears at the member  $i$  with the minimum of  $C_{Ri}/C_{RBAi}$  particularly in S structures (including the S type (S-3) of SRC structure). And when  $C_{Ri}$  is larger,  $\beta$  tends to be greater. It is noted that, for S pattern of the RC structure,  $\beta$  has rather uniform distributions when  $C_{Ri}/C_{RBAi}$  is relatively small in the middle member, while  $\beta$  becomes greater at middle stories when  $C_{Ri}/C_{RBAi}$  is uniform, i.e., pattern M.

In all the examples of the RC structure, seismic margin indices for member approach relatively uniform distributions, in comparison with those of S and SRC structures.

#### 3.2 Relation between seismic hazard and $\beta$

The relation between the mean of 50-year maximum peak ground acceleration  $\tilde{a}$  and  $\beta$  are shown in Fig.5. It may be seen that, except for the model L-3 of SRC(●)

structure,  $\beta$  decreases as  $\tilde{a}$  increases. The building constructed at a site with low earthquake seismic hazard tends to have a greater safety margin.

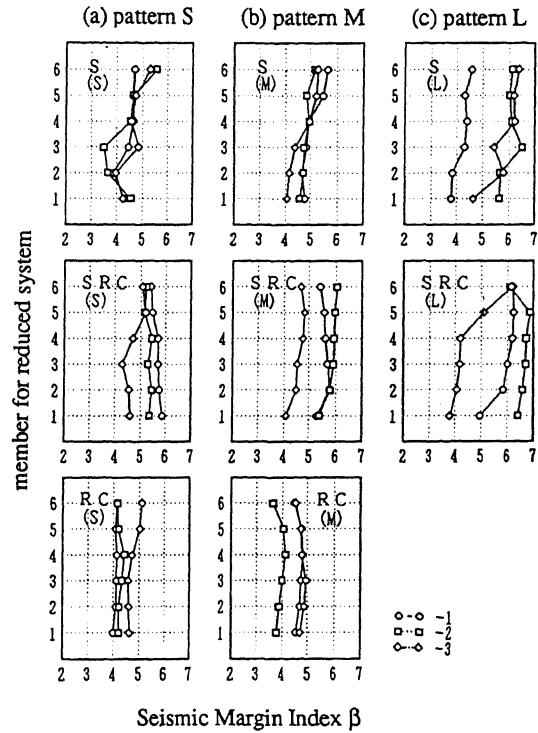


Fig.4 Vertical Profile of Seismic Margin Index  $\beta$

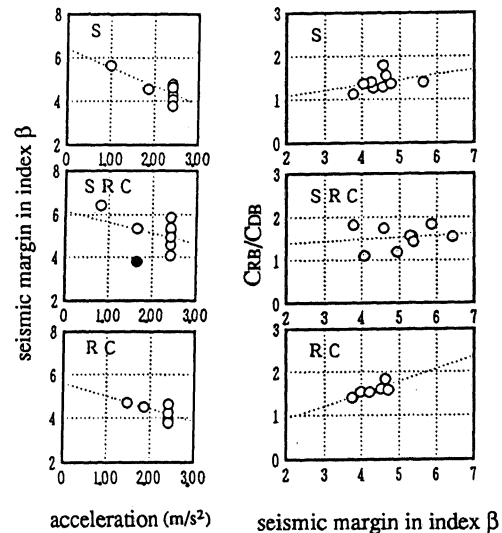


Fig.5 Relation between seismic hazard and  $\beta$

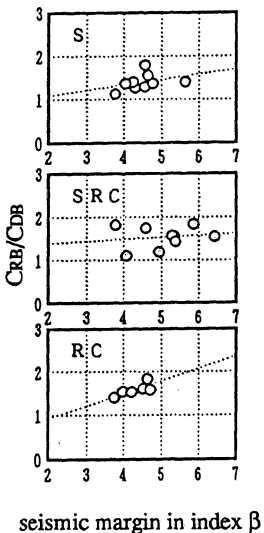


Fig.6 Ratio of base shear force coeff. and  $\beta$

### 3.3 Relation between base shear force coefficient and $\beta$

In order to find out the effect of the difference between structural resistance and input level on index  $\beta$ , we examined the design base shear force coefficient ratio defined as  $C_{RB}/C_{DB}$ .

Its relation to  $\beta$  of the 1st member is plotted in Figure 6. It can be noticed that a positive correlation between  $C_{RB}/C_{DB}$  and  $\beta$  holds for S and RC structures, i.e., safety index  $\beta$  for the 1st member increases with the ratio  $C_{RB}/C_{DB}$ , but this is not clear for SRC structures.

### 4 Conclusions

It can be concluded that the seismic margin index for members varies corresponding to different yield-shear-force coefficient distributions. For steel structures,

especially for the S pattern yield-shear-force coefficient distributions (smaller than the Ai distribution), the seismic margin index is smaller for the middle-lower members, while for other patterns (similar to and larger than the Ai distribution) the seismic margin index for members gradually increases with height. For RC structures, the distribution of the seismic margin index is fairly uniform irrespectively with yield-shear-force coefficient distribution patterns. The relation of both the base shear coefficient values and the seismicity to the seismic safety is also clearly demonstrated.

### ACKNOWLEDGMENT

This study was financially supported by the Ministry of Education, under Grant-in-Aid for Scientific Research, No.01302047.

### REFERENCES

- "Building standard law enforcement order", 1986 pp134 (in Japanese)
- Dan & J.kanda, 1986, A seismic risk study based nonempirical extreme value distribution, Trans.AIJ no.363, pp50.(in Japanese)
- Jennings, P., Housner, G. and Tsai, 1968, N.C., Simulated earthquake motions, Earthq. Engr. Res. Lab. California Inst.
- Kanai, K, An empirical formula for the spectrum of strong earthquake motions, 1961, Bull. Earthq. Res. Inst., Univ. of Tokyo, 39, 85-95
- Kanda, J & Iwasaki, R, 1987, Practical measure of probability-based seismic safety for inelastic building structures, Proc. JCOSSAR, pp.183-188
- Kanda, J & Iwasaki, R, 1988, Stochastic evaluation of inelastic seismic response for multi-degree-of freedom lumped mass models, Proc. 9WCEE, vol. VIII-797-802.
- Zhang S.H. & J.Kanda, 1990, Variation of yield-shear-force-coefficient distribution of existing tall buildings, Tech. Papers. Annual meeting. Japan, pp593 (in Japanese)
- Zhang, S.H., J.Kanda & R.Iwasaki, 1991, Effect of yield force coefficient distribution on evaluation of the seismic capacity of existing high rise building, Tech. Papers. Annual meeting. Japan, pp85. (in Japanese)

Table 1 The data of the analyzed buildings

structure	model	site	base shear coef.		reference input level $a_0(m/s^2)$	mean value 50-year max $(m/s^2)$
			CDB	CRB		
S	S-1	Tokyo	0.118	0.149	3.59	2.43
	S-2	Osaka	0.120	0.155	4.36	2.43
	S-3	Tokyo	0.160	0.226	4.41	2.43
	M-1	Kanagawa	0.130	0.178	3.86	2.43
	M-2	Nigada	0.079	0.142	3.68	2.43
	M-3	Tokyo	0.144	0.100	4.46	2.43
	L-1	Tokyo	0.165	0.274	3.62	2.43
	L-2	Hokaido	0.150	0.210	4.37	1.00
	L-3	Tokyo	0.150	0.233	2.54	2.43
SRC	S-1	Tokyo	0.135	0.194	0.74	2.43
	S-2	Saitama	0.140	0.125	0.82	1.65
	S-3*	Osaka	0.160	0.277	4.28	2.43
	M-1	Tokyo	0.084	0.132	0.52	2.43
	M-2	Tokyo	0.100	0.143	0.79	2.43
	M-3	Nagoya	0.153	0.168	0.63	2.43
	L-1	Kanagawa	0.130	0.154	0.76	3.29
	L-2	Fukuoka	0.101	0.116	0.57	0.82
	L-3*	Hiroshima	0.128	0.233	3.98	1.65
RC	S-1	Tokyo	0.145	0.224	0.72	2.43
	S-2	Tokyo	0.130	0.199	0.88	2.43
	S-3	Tokyo	0.120	0.221	1.17	2.43
	M-1	Nigata	0.110	0.178	0.79	1.86
	M-2	Tokyo	0.085	0.119	0.81	2.43
	M-3	Mie	0.110	0.174	0.85	1.48

\* S type in the SRC structures

Table 2. Shape of the  $\beta$ -value's vertical distribution

pattern	S and S type in the SRC structures	RC and RC type in the SRC structures
pattern S	small in the lower-middle members	roughly same for all the member
pattern M	distribution roughly same generally smallest in the leeriest member	larger in the middle members
pattern L	larger beyond the second member, smallest in the leeriest member	generally smallest in the 1st member